FLUX RATIO AND DRIVING FORCES IN A MODEL OF ACTIVE TRANSPORT

R. BLUMENTHAL *and* O. KEDEM

From the Polymer Department, Weizmann Institute of Science, Rehovot, and Nuclear Research Centre-Negev (Israel Atomic Energy Commission), Negev, Israel

ABSTRACT In order to analyze the energetics of active transport, a hypothetical carrier model is considered in which the active transport process is reduced to a minimal number of elementary steps. The relation between the following three quantities is examined: The affinity of the reaction driving the active transport, the ratio of isotope fluxes between identical solutions ("short-circuit"), and the maximal chemical potential difference which the active transport system can maintain. The interdependence of isotope interaction and the degree of coupling between transport and chemical reaction is shown explicitly: when the transport and chemical reaction are completely coupled, there is marked isotope interaction. In general, the logarithm of the short-circuit flux ratio (multiplied by RT) and the maximal chemical potential are not equal. The two quantities are approximately equal, when coupling between metabolism and transport is very loose, or when the reaction step is much faster than the transfer of the adsorbed solute across the barrier. Without prior knowledge of the kinetic parameters of the carrier, the maximal potential and the dependence of the metabolic reaction on solute flow have to be measured in order to derive the affinity of the driving reaction. Measurement of the flux ratio in the same system will then yield independent information on the carrier mechanism.

INTRODUCTION

The metabolic "driving force" of active transport has so far not been accessible to direct investigation. Information on the energetics of active transport systems is obtained from the fluxes of the transported species, their response to potential gradients, and, wherever possible, the dependence of the rate of metabolism on the rate of transport.

The metabolic "pump" can build up, and maintain, a maximal electrochemical potential difference for the transported species; at this point the rate of transport vanishes. Emphasizing the analogy to an electrochemical cell, the potential of zero sodium flow for a system actively transporting sodium, was termed E_{Na}(1). The measurement of E_{Na} provides information on the affinity of the coupled metabolic reaction, although the relation cannot be expected to be as simple as in a battery.

In his analysis of tracer fluxes, which made the detailed study of ion transport

possible, Ussing (2) gave another definition of E_{Na}, $E_{Na} = (RT/F) \ln f^{sc}$, where f^{sc} is the sodium flux ratio between identical solutions at short circuit. Ussing (2) and other authors pointed out that a number of simplifying assumptions underlie this definition.

A general analysis of forces and flows shows that the two operationally defined quantities, the electrochemical potential difference at zero flow and the flux ratio at short circuit, are not a priori identical (3). Even if the influence of other processes, like solvent drag, is allowed for, different parameters determine $(\Delta\tilde{\mu}_{Na})_{J_{Na}=0}$ and $RT \ln f^{sc}$. Experimentally, different values have been obtained for these quantities (see reference 2, p. 122). In the following these parameters are compared in a carrier model for active transport. The main purpose is not the specific analysis of the model chosen here, but the reexamination of relations which have been assumed to hold for active transport systems in general.

For the sake of simplicity, the transported species is a nonelectrolyte, so that we are considering a gradient of chemical potential only, and the analogy with a battery is thus not so obvious. The chemical potential difference between two sides of the membrane at zero flow, however, is completely analogous to the electromotive force of a battery and the model system may serve for a detailed discussion of the problem. Thus, the driving force of the active transport pump (the affinity of the reaction) will be compared with the logarithm of the flux ratio at vanishing chemical potential difference of transported species ($(RT \ln f)_{\Delta\mu=0}$), and with the maximal chemical potential difference the active transport pump can reach at vanishing rate of transport; ($(\Delta\mu)^o$).

The Model

As a plausible example of a carrier which mediates active transport we propose an expanding and contracting protein within the membrane. The protein is assumed to have one binding site for the transported species, which shuttles back and forth across the membrane, and a second binding site on the inner side of the membrane, which serves as a catalytic site for the reaction (substrate → product). This protein then acts as a little machine inside the membrane, performing a number of functions. In a real system the function could well be distributed over a number of cell components and the chemical reaction would consist of a sequence of reactions. We shall indiscriminately designate the protein as "carrier" or "protein," according to its function.

Our model belongs to a class of models for uphill carrier transport (4). In the model described by Rosenberg and Wilbrandt the reaction driving the active transport takes place on both sides of the membrane[1], while in our model the reaction takes place on the inner side of the membrane only, and substrate and product do

[1] The membrane "pump" asymmetry is still maintained since different reactions take place on both sides of the membrane.

not permeate. This is in agreement with the concept that the cell regulates the rate of transport, or the concentration of the transported species, from the inside. By means of metabolic feedback mechanisms a certain value for the inner concentrations of substrate and product is "chosen," and consequently the maximal chemical potential will be determined. It is assumed that water flow does not interact with the flow of the actively transported species, F.

In the absence of substrate the protein may exist in the four states shown schematically in Fig. 1 a. The possible transitions between these four states and their probabilities are indicated in Fig. 1 b. Here k_{ij} is the rate constant for transition $i \rightarrow j$, and $F_{i,o}$ the concentrations of F in the inner and outer compartments. We are thus considering first order processes only, and assuming that the rate of adsorption of a solute is proportional to its concentration. At equilibrium, microscopic reversibility requires balance for each step separately, and thus the k_{ij}'s are not independent:

$$N_3k_{31} = N_1k_{13}F_i \qquad N_2k_{21} = N_1k_{12}$$
$$N_3k_{34} = N_4k_{43} \qquad N_2k_{24}F_0 = N_4k_{42}\,. \tag{1}$$

N_i denotes the number of carrier molecules in state i, per square centimeter of membrane surface. Since, at equilibrium, $F_o = F_i$, equation 1 gives

$$k_{12}k_{24}k_{43}k_{31} = k_{13}k_{34}k_{42}k_{21} \equiv a. \tag{2}$$

In the cyclic process, the clockwise product of rate constants is equal to the anticlockwise product.

The kinetics of such a facilitated transport system have been reported previously (5).

The model system will carry out active transport by means of the following mechanism (Fig. 2 a): Substrate binds to the contracted protein (state 5) and inter-

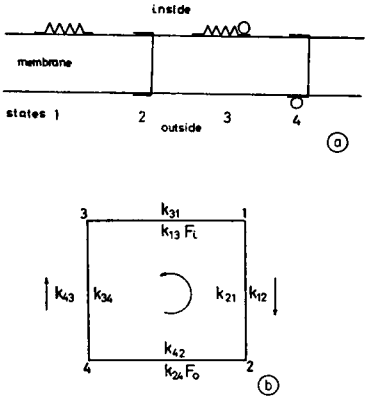

FIGURE 1 a. The possible states of the carrier-protein mediating solute transport. Circle, transported species. b. Transitions between states 1 to 4. Frequencies of transitions in the clockwise direction are indicated on the outside of the cycle, anticlockwise transitions on the inside.

acts with the binding site for the transported species, thereby excluding any further binding. The substrate-protein complex expands (state 6), thereby drawing the substrate closer to the catalytic site and enabling it to undergo chemical reaction. Through this reaction, a product is formed (state 8) which instantaneously dissociates from the protein.

In Fig. 2 b, which gives the kinetic diagram corresponding to the states in 2 a, S denotes the concentration of substrate, and P the concentration of product, both of them present inside only. Transitions between states include a first-order chemical reaction ($6 \leftrightarrows 8$). In Figs. 1 and 2, the stretched states are denoted for convenient reference by even numbers, and the contracted states by odd numbers; in odd-even transitions the adsorption site crosses the membrane.

The contractile protein can go through three cyclic sequences of states, represented in Fig. 2 b. In cycle *a* (12431), one molecule of F is transferred across the membrane; in cycle *b* (156821), one molecule of substrate is transformed into product; in cycle *c* (15682431), one molecule of F is taken up, and one molecule of substrate is consumed. It is this sequence of states which gives rise to coupling between transport and reaction. If the protein cannot expand or contract when "unloaded" (i.e. without adsorption of transported species or substrate), then the transition 1–2 is impossible and only the large cycle *c* remains (Fig. 3 a). In this case the reaction would be completely coupled to the transport. If, however, this

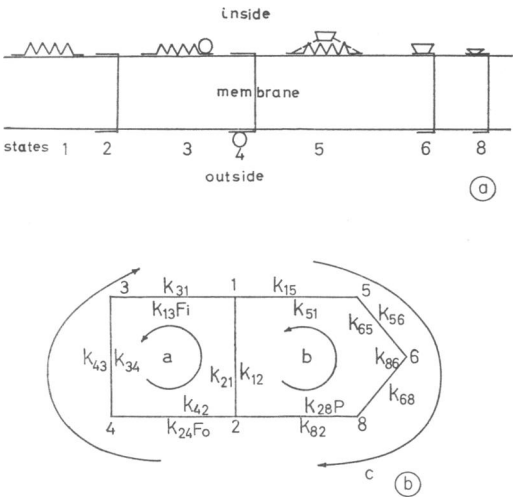

FIGURE 2 a. The possible states of the carrier-protein mediating active transport. Quadrangle, substrate; inverted triangle, product, and circle, transported species. b. Transitions between the states in 2 a and their frequencies.

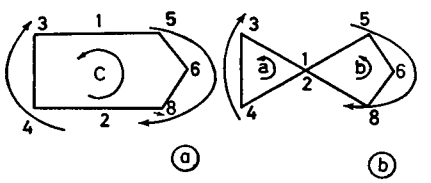

FIGURE 3 a. Complete coupling and b uncoupling between transport and reaction.

transition is instantaneous, so that 1 and 2 merge into one state, the two processes become entirely independent (Fig. 3 b).

At chemical equilibrium,

$$P^{equ}/S^{equ} = K \tag{3}$$

and microscopic reversibility leads to a cycle product for cycle b

$$k_{15}k_{56}k_{68}k_{82}k_{21} = k_{12}k_{28}k_{86}k_{65}k_{51}K \equiv b. \tag{4}$$

As cycle c covers cycles a and b, except the tie line 1–2, the three cycle products are related by

$$c = \frac{ab}{k_{12}k_{21}}. \tag{5}$$

Flows during Active Transport

In a stationary state the rate of reaction per square centimeter is given by the rate of conversion of 1 mole of protein in state 6 into one molecule of protein in state 8: $(k_{68}N_6 - k_{86}N_8)$. Similarly the rate of uptake of transported species per square centimeter is given by $k_{31}N_3 - k_{13}F_iN_1$ (cf. Fig. 2). The expressions for the N_i's in the stationary state may be obtained by simultaneously solving a set of algebraic equations, namely

$$\sum_{i=1}^{n} N_i = N_t \tag{6}$$

and one equation for each protein state, $(dN_i/dt = 0)$. The solution of this set of equations is straightforward, but very tedious, even when the determinant method (i.e. Cramer's rule) is employed.

More powerful methods for the evaluation of reaction rates in complex enzyme reaction sequences (6) and of steady-state fluxes for unimolecular systems (7) have been developed, using cyclic diagrams as an essential tool in the calculation.

According to Hill's diagram method (7), one derives the frequency of each cycle, at the given driving forces, from a series of "flux diagrams." Each flow can be written as a sum of all cycles "contributing" to it. Clearly, in the present model, cycles a and c contribute to transport, cycles b and c to reaction. The flux diagrams are given in the Appendix—here we shall write down the contribution of each cycle and the flows. As we are interested in the ratios between flows only, we shall omit a constant containing a sum of products of the rate coefficients, and consider re-reduced flows. The relation between the flows J_i, and the reduced flows, j_i, is given in the Appendix.

At least two isotopes of the transported solute, F, have to be considered for the investigation of flux ratios. Assuming the outer compartment to contain isotope 1

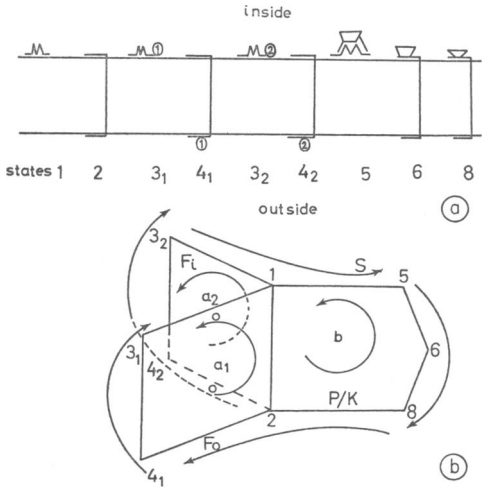

FIGURE 4 The possible states (Fig. 4 a) of the carrier-protein in the presence of two different isotope species (1) and (2). Quadrangle, substrate; inverted triangle, product. Figure 4 b shows the possible transitions between the states. Only concentration-dependent transition probabilities are indicated.

only and the inner compartment isotope 2 only, the flow j_1 of isotope 1 is then the "influx" of transported species, the flow $-j_2$ of isotope 2 is the "outflux,"[2] and $j_1 + j_2$ the net flux. The outer concentration of isotope 1 is thus equal to the over-all outer concentration of transported species, $F_1^o = F^o$, and the inner concentration of isotope 2 equals its over-all inner concentration $F_2^i = F^i$. With two isotopes the protein can assume nine instead of seven states (Fig. 4 a), so that the protein, loaded with transported species, assumes four different states; 3_1 and 4_1 for the contracted and expanded protein-isotope 1 complex, and 3_2 and 4_2 for the contracted and expanded protein-isotope 2 complex (Fig. 4 b).

Both cycles, a and c, are now each split into two cycles running parallel (cf. Figs. 4 b and 5; only the concentration-dependent transition probabilities are indicated in these figures). Since we assume that F_1 and F_2 are identical in their thermodynamic and kinetic properties (except radioactivity), all rate constants are identical in a_1 and a_2 ($a_1 = a_2 = a$) and in c_1 and c_2 ($c_1 = c_2 = c$). The frequencies of the cycles, however, depend also on F_1 and F_2, respectively.

By splitting the cycle a we have created a new cycle, a_{12}, in which the protein goes through the states $(24_13_113_24_22)$. Cycle a_{12} brings about exchange of F_1 and F_2 without contributing to either net flow or reaction. In other words, exchange diffusion occurs, since the flux cycles of both isotopes are hinged onto the same reaction cycle. Going around cycle a_{12}, we cover cycles a_1 and a_2 except the tie line 1–2, and hence:

$$a_{12} = a^2/(k_{12}k_{21}). \tag{7}$$

[2] In practice one uses one abundant isotope present on both sides of the membrane and two tracer species, each present on one side of the membrane only. Influx and outflux are then defined as j^*/ρ^* and $-j^{**}/\rho^{**}$ where ρ^* and ρ^{**} are the ratios between the concentrations of the tracers and the abundant species. Both procedures will give identical results if all isotope effects are negligible.

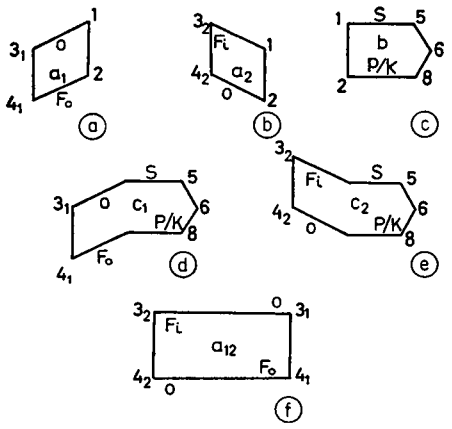

FIGURE 5 The separate cycles corresponding to the basic diagram in Fig. 4 b. Only concentration-dependent transition probabilities are indicated. O indicates absence of isotope 1 inside and of isotope 2 outside.

The coupling between j_1 and j_2 (isotope interaction) will be tight if the transition 1–2 is slow compared to the other steps in cycles a_1 and a_2. This is also a condition for tight coupling between reaction and transport. In this type of model, efficient active transport and isotope interaction go together.

The reaction rate is given by line 6–8 (Fig. 4 b) and this line is part of cycles b, c_1, and c_2. The reaction rate, j_r, is then composed of the three contributions:

$$j_r = (j_b + j_{c_1} + j_{c_2}). \tag{8}$$

The line 2–4_1 (Fig. 5 b) gives the flow of isotope 1 and is used by cycles a_1, c_1, and a_{12}:

$$j_1 = (j_{a_1} + j_{c_1} - j_{12}). \tag{9}$$

Similarly,

$$j_2 = (j_{a_2} + j_{c_2} + j_{12}). \tag{10}$$

Maximal Potential and Flux Ratio

In terms of the separate cycles, the net flux is given by

$$j = j_1 + j_2 = j_{a_1} + j_{a_2} + j_{c_1} + j_{c_2}. \tag{11}$$

The fluxes of the transported species are taken positive from the outside to the inside. Inserting the expressions for the cycles given in the Appendix (A-6) into equations 11 and 8 and rearranging, we obtain for the reduced net flow and reaction flow.

$$j = F_iS[1 + (k_{12}/k_{56})(K_S\theta_S/S)](F_0/F_i - 1) + F_iS(1 - P/KS) \tag{12}$$

$$j_r = F_iS(F_0/F_i - 1) + SF_i[1 + (k_{12}/k_{34})(K_F\theta_F/F_i)](1 - P/KS). \tag{13}$$

K_S and K_F are the dissociation constants for the carrier–substrate complex and for the carrier–F complex. θ_S and θ_F are combinations of rate constants, given in the Appendix. Both are larger than 1; for fast adsorption-desorption of F, $\theta_F = 1$. θ_S reduces to unity only if the chemical reaction as well as adsorption-desorption is fast as compared to carrier-transfer.

The thermodynamic driving forces, conjugate to the chemical reaction and the solute flow, are the affinity, A, and the difference of thermodynamic potential, $\Delta\mu$ (8). In ideal solution

$$\Delta\mu = \mu_F^o - \mu_F^i = RT \ln F_o/F_i$$

and

$$A = RT \ln SK/P.$$

Near equilibrium, when concentrations of F are not widely different and substrate and product concentrations are near the equilibrium ratio,

$$\ln F_o/F_i \simeq F_o/F_i - 1 \quad \text{and} \quad \ln SK/P \simeq 1 - P/SK. \tag{14}$$

Thus, near equilibrium, equations 13 become linear force-flux relations of the form

$$\begin{aligned} j &= l_{11}\Delta\mu + l_{12}A \\ j_r &= l_{21}\Delta\mu + l_{22}A \end{aligned} \tag{15}$$

in which the Onsager relation is obeyed: comparison of equations 12, 13, and 15 shows that $l_{12} = l_{21}$.

From general thermodynamic considerations,

$$l_{12}^2 \leqslant l_{11}l_{22}.$$

In strongly coupled systems, the cross-coefficients are relatively large. The degree of coupling, q, between one reaction and one solute flow is defined by (9)

$$\left(\frac{j_r}{j}\right)_{A=0}\left(\frac{j}{j_r}\right)_{\Delta\mu=0} = q^2 = l_{12}^2/l_{11}\,l_{22}. \tag{16}$$

For tight coupling $q^2 \to 1$, for uncoupled flows $q^2 = 0$. Substituting the coefficients from Equations 12 and 13 into Equation 16

$$q^2 = \frac{1}{(1 + R_S/S)(1 + R_F/F)}, \tag{17}$$

where

$$R_S = (k_{12}/k_{56})K_S\theta_S$$

$$R_F = (k_{12}/k_{34})K_F\theta_F . \tag{18}$$

Evidently, when the conformational transition of unloaded carrier (transition 1–2) is slow compared to that of the carrier complex with either F or S (transitions 3–4 and 5–6), the process is tightly coupled ($q^2 \rightarrow 1$). When, on the other hand, the movement of the unloaded carrier is relatively fast (i.e. the carrier "slips" without transport or reaction) the coupling vanishes ($q^2 \rightarrow 0$). Alternatively, tight coupling may also occur at saturation concentrations of substrate and transported species. Since at saturation the rate of transport becomes very low, the fact that tight coupling occurs is trivial. Low concentrations of substrate and of transported species tend to decrease the degree of coupling.

Net flow vanishes when the thermodynamic potential gradient is balanced by the affinity of the coupled reaction. From Equations 12 and 18 the value of $\Delta\mu$ at zero net flow is,

$$(\Delta\mu)^0 = (RT \ln F_o/F_i)_{j=0} = -RT \ln \frac{S + R_S}{P/K + R_S} . \tag{19}$$

The expressions for the flows of isotopes 1 and 2 are derived by inserting expressions for the individual cycles (equation A-6 into 9 and 10), and introducing R_S and R_F according to equation 18

$$j_1 = [S + R_S + (R_S/R_F)F_i]F_o$$

$$j_2 = -[P/K + R_S + (R_S/R_F)F_o]F_i . \tag{20}$$

The flux ratio is given by

$$f = -j_1/j_2 = \frac{F_o}{F_i} \frac{S + R_S + (R_S/R_F)F_i}{P/K + R_S + (R_S/R_F)F_o} . \tag{21}$$

The logarithm of the flux ratio at "short circuit" ($F_i = F_o$) is then

$$RT \ln f^{sc} = RT \ln \frac{S + R_S + (R_S/R_F)F}{P/K + R_S + (R_S/R_F)F} . \tag{22}$$

Evaluation of the Affinity

Equations 21 and 22 show that both $(\Delta\mu)^o$ and $RT \ln f^{sc}$ are smaller than the affinity, ($A = RT \ln KS/P$). Furthermore, $| RT \ln f^{sc} | < | (\Delta\mu)^o |$. This inequality is in agreement with experimental observations on a number of active transport systems.

If $R_S/S \ll 1$, the chemical potential difference $(\Delta\mu)^o$ is equal to the affinity. If, in addition, the reaction step is much faster than the transport part of the cycle, $R_S/R_F \ll 1$, then $RT \ln f^{sc} \mid \rightarrow \mid (\Delta\mu)^o \mid \rightarrow \mid A$. The same result will be obtained if F is very small; in this case the molecules of the transported species do not have to "queue" for transfer by the reaction. Although exchange diffusion is possible in this carrier system, its contribution to isotope flux will be small under the conditions of the experiment.

If the unloaded carrier crosses the barrier readily, R_S may become large enough to make the last term in numerator and denominator in equation 21 negligible. In this case $RT \ln f^{sc} = (\Delta\mu)^o$, and both are considerably smaller than A. The system is then loosely coupled (cf. equation 18) and cannot efficiently carry out uphill transport.

In the linear range the affinity can be derived from two independent measurements. From equation 15, the affinity is given by the maximal potential $(\Delta\mu)^o$ and by the dependence of substrate consumption on the flow:

$$A = -(\Delta\mu)^o(\partial j_r/\partial j)_A . \tag{23}$$

For the carrier model one obtains, near equilibrium:

$$(\Delta\mu)^o = -\frac{S}{R_S + S} A \tag{24}$$

$$(j_r/j)_A = \frac{S}{R_S + S} . \tag{25}$$

It can be shown that, for the carrier model, equation 23, is a good approximation in the nonlinear range.

Stoichiometry

The inherent stoichiometry for the carrier model described here is 1:1, i.e. 1 mole of F may be transported for 1 mole of S consumed, if there is no "slip." In terms of the elementary cycles contributing to the process, j_c gives rise to the 1:1 active transport, whereas cycles a and b comprise independent pathways which will modify the ratio j/j_r under various conditions.

For an experimental determination of stoichiometry of active transport, two types of measurements are possible in principle, and have been carried out in a few systems:

(a) flow of transported species per mole of reaction, $(j/j_r)_{\Delta\mu=0}$

(b) response of metabolism to a change of j, dj_r/dj.

For the carrier model we obtain from equations 15 and 16.

$$(j/j_r)_{\Delta\mu=0} = \frac{1}{1 + R_F/F} . \tag{26}$$

The ratio is in general smaller than 1 and approaches unity, if $R_F \to 0$. Thus method *a* would lead to an underestimate of the stoichiometric ratio.

In order to draw conclusions from the measurements of chemical reaction as a function of transport, it is essential to define the restriction imposed on the system. Constant affinity was assumed and the partial derivative $(\partial j_r/\partial j)_A$ was used above in order to derive the affinity in incompletely coupled systems. The affinity may be kept constant, either artificially, by introducing large reservoirs for substrates and products or, in living cells, by metabolic regulatory mechanisms. The net flow (j) may then be varied by changing $\Delta\mu$.

From equation 24 it is seen that $\left(\frac{\partial j}{\partial j_r}\right)_A > 1$. Using this derivative as a measure of stoichiometry (method *b*), one would arrive at an overestimate of moles transported per mole metabolite consumed. Only for complete coupling ($R_S \to 0$):

$$\left(\frac{\partial j_r}{\partial j}\right)_A = \left(\frac{j}{j_r}\right)_{\Delta\mu=0} = 1$$

In general (cf. equations 24, 26, and 18)

$$(j/j_r)_{\Delta\mu=0}\,(\partial j_r/\partial j)_A = \frac{1}{(1 + R_S/S)(1 + R_F/F)} = q^2 < 1. \qquad (27)$$

If there are no large reservoirs, nor regulatory mechanisms to keep A constant, an increase in j will tend to run down A, decreasing further the derivative dj_r/dj. From equations 15 and 16:

$$dj_r/dj = (\partial j_r/\partial j)_A + l_{22}(1 - q^2)\,(dA/dj) \qquad (28)$$

Since $dA/dj < 0$, dj_r/dj is smaller than $(\partial j_r/\partial j)$ at constant affinity.

Isotope Interaction

It is clear from inspection of the model and from equations 9 and 10 that the flows of the two isotopes are coupled: flow of one of the isotopes in one direction enhances the flow of the other in the opposite direction by exchange diffusion, (cycle j_{12}). It has been shown previously (3, 4) that the ratio between permeability to isotope exchange (ω^*) and to net flow (ω), is determined by this interaction between isotope flows.

The reduced permeability coefficients are defined by:

$$\omega^* = (j_2/\Delta F_2)_{j_r=0,j=0}$$

$$\omega = (i/\Delta F)_{j_r=0}. \qquad (29)$$

The relation between these coefficients and the actual permeability coefficients is

analogous to the relation between the reduced flows and the value of J_i. The permeability for self-diffusion is obtained by introducing equation 19 into 29, with $F = F^o$ and $S = P/K$

$$\omega^* = S + R_S + (R_S/R_F)F. \tag{30}$$

The permeability coefficient for net flow, ω, is obtained directly from equations 12 and 13.

$$\omega = (j/F)_{j_r=0} = \frac{S + R_S + (R_S/R_F)F}{1 + F/R_F}. \tag{31}$$

If both permeability coefficients are measured under similar conditions, the ratio of permeabilities is:

$$\omega^*/\omega = 1 + F/R_F. \tag{32}$$

The same result has been obtained (5) for passive carrier-mediated transport.

The isotope interaction will vanish ($\omega^*/\omega = 1$) when the resistance of the exchange cycle is large; the system will then be shunted by the transitions of unloaded carrier (k_{12}).

CONCLUSIONS

1. A carrier model for active transport may be represented by a basic diagram consisting of two cycles: a transport cycle and a reaction cycle. The coupling between reaction and flow is determined by the "slip" of the free carrier. Fast transition of free carrier uncouples transport and reaction.

2. In the presence of isotope flows a third cycle is added onto the basic diagram. The presence of this third cycle introduces exchange diffusion, which gives rise to isotope interaction.

3. Isotope interaction is also determined by the relative frequency of transition of the free carrier. There is thus an indirect relation between degree of coupling and isotope interaction.

4. The following relation was obtained between flux ratio, affinity, and $(\Delta\mu)^o$:

$$| RT \ln f^{sc} | \leqslant | (\Delta\mu)^o | \leqslant | A |.$$

5. In two cases $RT \ln f^{sc}$ and $\Delta\mu^o$ become equal: (*a*) when coupling between reaction and transport is loose; (*b*) when the reaction pathway is much faster than the transport pathway.

6. In general, both $(\Delta\mu)^o$ and the dependence of the metabolic reaction on solute flow $(\partial j/\partial j_r)_A$ have to be measured in order to derive the affinity. Measurement of $RT \ln f^{sc}$ yields independent information on the carrier mechanism.

7. The apparent stoichiometry of the active transport system is dependent on the conditions of measurement. In the model described here the inherent stoichiometry is 1:1. Measurement at "short-circuit" conditions ($\Delta\mu = 0$) gives $(j/j_r)_{\Delta\mu=0} < 1$, while measurement of metabolism as function of flow leads to $(\partial j/\partial j_r)_A > 1$.

8. Experimentally, affinity may be kept constant either artificially, by introducing large reservoirs for substrate and product, or by metabolic regulatory mechanisms. If these conditions are not fulfilled, (dj_r/dj) will be measured, which is smaller than $(\partial j_r/\partial j)_A$.

APPENDIX

We shall follow the method developed by Hill for obtaining steady fluxes directly from the diagram. These fluxes are given by the difference of transition frequencies along a line in a diagram (Fig. 2 a). This device is especially convenient if one is interested in the ratios between the flows and not in their absolute values.

According to Hill, first the "flux diagrams" for all possible cycles are drawn. Each flux diagram consists of one closed cycle and the maximal number of lines leading into the cycle without forming a second cycle.

The possible flux diagrams for cycle a are:

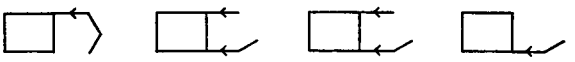

(A-1)

and for cycle b:

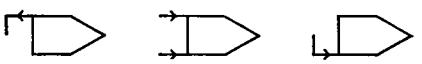

In a nonequilibrium stationary state the number of transitions i to j will be different from those in the opposite direction. The corresponding transition probabilities are written on both sides of the line, the inside and outside of the cycle (Fig. 2), and the round arrows indicate the direction. A directed line in the flux diagrams represents one transition probability only, and the correspondence between directed lines and the coefficients in the basic diagram (Fig. 2) is obvious. The algebraic expression corresponding to a flux diagram is given by the difference between the clockwise and anticlockwise products of transition probabilities for the complete cycle. This difference is then multiplied by the transition probabilities indicated by the directed lines leading into the cycle. A "cycle" is given by the sum of its flux diagrams, whereas a steady-state flow is given by:

$$J_{i\to j} = \frac{N_i \times \text{sum of cycles using transition } i \to j.}{\Sigma}. \qquad \text{(A-2)}$$

The denominator Σ denotes a sum which appears in all flows for a given model and thus cancels in the ratios.

The "cycles" corresponding to a, b, and c (cf. Fig. 2) are the following:

$$\begin{aligned} J_a &= a\beta(F_o - F_i) \\ J_b &= b\alpha(S - P/K) \\ J_c &= c(SF_o - PF_i/K). \end{aligned} \qquad \text{(A-3)}$$

The factors a, b, and c are products of transition probabilities within the closed cycles, given by equations 4, 5, and 6. The factors α and β are products of transition probabilities flowing into the cycles and are obtained by summing the flux diagrams of a and b (equation A-1).

$$\alpha = k_{31}\, k_{42}\left(1 + \frac{k_{43}}{k_{42}} + \frac{k_{34}}{k_{31}}\right) = k_{13}\, k_{42}\, K_F\, \theta_F\,, \qquad \text{(A-4)}$$

$$\beta = k_{51}\, k_{68}\, k_{82}\left(1 + \frac{k_{56}}{k_{51}} + \frac{k_{65}}{k_{68}} + \frac{k_{65}\, k_{86}}{k_{82}\, k_{68}}\right) = k_{15}\, k_{68}\, k_{82}\, K_S\, \theta_S\,. \qquad \text{(A-5)}$$

In these expressions $K_F = k_{31}/k_{13}$ and $K_S = k_{51}/k_{15}$ are the dissociation constants of the contracted protein-transported species complex and contracted protein-substrate complex, whereas θ_F and θ_S are constants defined, respectively, by equations A-4 and A-5. If the adsorption-desorption processes are fast as compared to the membrane crossing ($k_{43} \ll k_{42}$, $k_{34} \ll k_{31}$), θ_F reduces to unity. θ_S may still be large, if the reaction step is slow ($k_{68} \ll k_{65}$).

According to equation A-3, each cycle is proportional to a concentration difference, giving rise to a driving force. The line 6-8 measuring the chemical reaction is part of cycles b and c, whereas line 3-1, representing uptake of the transported species, is part of cycles a and c (Fig. 2). In the case of isotope flows during active transport we have to consider the flux diagrams corresponding to the cycles in Fig. 5. These are similar to those given by equation A-1, but the number of directed lines flowing into the cycles is multiplied by the presence of the second cycle a. The "cycles" a_1, a_2, b, c_1, and c_2 therefore contain the additional factor α.

Our interest lies in the reduced values only, and we shall therefore, not evaluate Σ. It will further be found convenient to divide all flows by $c\alpha$. Reduced flows, j_i, will be defined as:

$$j_i = \frac{J_i\, \Sigma}{N_t\, c\alpha}\,.$$

Taking expressions for a, b, c, a_{12}, α and β from equations 2, 4, 5, A-4, and A-5 the reduced flows become:

$$j_{a_1} = (a\beta/c)F_o = (k_{12}/k_{56})K_S\, \theta_S\, F_o$$

$$j_{a_2} = -(a\beta/c)F_i = -(k_{12}/k_{56})k_S\, \theta_S\, F_i$$

$$j_b = (\alpha b/c)(S - P/K) = (k_{12}/k_{34})k_F\theta_F(S - P/K)$$

$$j_{c_1} = SF_o \qquad j_{c_2} = -(P/K)F_i$$

$$j_{12} = -\frac{a^2\beta}{k_{12}\, k_{21}\, \alpha c}\, F_i\, F_o = -\frac{k_{34}\, K_S\, \theta_S}{k_{56}\, K_F\, \theta_F}\, F_i\, F_o\,. \qquad \text{(A-6)}$$

From these individual cycles net flux, reaction rate, and isotope fluxes may be calculated.

REFERENCES

1. USSING, H. H., and K. ZERAHN. 1951. *Acta Physiol. Scand.* **23**:110.
2. USSING, H. H. 1961. The Alkali Metal Ions in Biology. Springer-Verlag OHG., Berlin.

3. KEDEM, O., and A. ESSIG. 1965. *J. Gen. Physiol.* **48**:1047.
4. ROSENBERG, T., and W. WILBRANDT. 1963. *J. Theoret. Biol.* **5**:288.
5. ESSIG, A., O. KEDEM, and T. L. HILL. 1966. *J. Theoret. Biol.* **13**:72.
6. WANG, J. T. F., and C. S. HANES. 1962. *Canad. J. Biochem. Phys.* **40**:763.
7. HILL, T. L. 1966. *J. Theoret. Biol.* **10**:442.
8. PRIGOGINE, I. 1967. Thermodynamics of Irreversible Processes. Interscience Publishers Inc., New York.
9. KEDEM, O., and S. R. CAPLAN. 1965. *Trans. Faraday Soc.* **61**:1897.